applied optics

Aberrational interactions between axial and lateral misalignments in pupil-offset off-axis two-mirror astronomical telescopes

Xiaoquan Bai,[1,2] Guohao Ju,[1,3] Hongcai Ma,[1,4] and Shuyan Xu[1]

[1]Changchun Institute of Optics, Fine Mechanics and Physics, Chinese Academy of Sciences, Changchun, Jilin 130033, China
[2]University of Chinese Academy of Sciences, Beijing 100049, China
[3]e-mail: juguohao@ciomp.ac.cn
[4]e-mail: hongcm@hotmail.com

Received 2 July 2019; revised 28 August 2019; accepted 29 August 2019; posted 29 August 2019 (Doc. ID 371378); published 23 September 2019

Due to the absence of rotational symmetry, the effects of axial and lateral misalignments couple tightly together, which leads to special aberration field characteristics. This paper will present an in-depth and systematic discussion on the interactions between the effects of axial and lateral misalignments in pupil-offset off-axis two-mirror astronomical telescopes. The aberration function of this class of telescopes in the presence of axial and lateral misalignments is derived. The specific expressions of two dominant non-rotationally symmetric aberrations, i.e., astigmatism and coma, are obtained and the aberration field characteristics are discussed. Importantly, it is shown that under certain conditions, a node will arise in the field of view for these two kinds of aberrations. Then the aberrational compensation mechanisms between axial and lateral misalignments are quantitatively explicated, and it is shown that the non-rotationally symmetric aberrations induced by axial misalignments can well be compensated by lateral misalignments. However, we also find that in this process, the defocus aberration induced by these two kinds of misalignments will accumulate (rather than cancel out). Therefore, in practice, it is better to separate these two kinds of misalignment. Finally, we propose a simple method to decouple axial misalignments from lateral misalignments with wavefront measurement at one field position. Most of this work can be extended to other kind of pupil-offset off-axis astronomical telescopes, such as off-axis three-mirror anastigmatic telescopes.

https://doi.org/10.1364/AO.58.007693

1. INTRODUCTION

Compared with on-axis astronomical telescopes, off-axis telescopes with an offset pupil do not have aperture obscuration caused by secondary mirror (SM) and its supporting structure; therefore, they have a higher energy-collection efficiency and better diffraction characteristics [1]. This fact means that off-axis telescopes have not only a higher resolution but also some advantages in ellipticity performance (an important parameter used to define the shape of a galaxy), which is of cardinal importance for weak gravitational lensing measurement (dark matter cannot be seen directly, but can be detected by weak gravitational lensing measurement) [2]. However, due to the absence of rotational symmetry, off-axis telescopes are more susceptible to mirror misalignments (when we refer to an "off-axis telescope," we particularly mean one in which the "parent" design has a single axis of rotational symmetry, but the entrance pupil is shifted sufficiently that the resulting system is unobscured) [3,4]. Furthermore, the aberration field characteristics of off-axis telescopes in the presence of misalignments are more complicated compared to those in on-axis telescopes. It is of great significance to present a deep discussion on the effects of misalignments in off-axis astronomical telescopes. An in-depth understanding of the aberration field characteristics induced by misalignments will contribute to the construction of this class of astronomical telescopes in many aspects.

Specifically, there are three main types of misalignments in off-axis astronomical telescopes, these being axial [5], lateral [6,7], and rotation misalignments [8]. Axial misalignments represent the dislocation of optical surfaces along the axial direction, lateral misalignments represent the decenter and tip–tilt of optical surfaces in the lateral direction, and rotational misalignments refer to the rotational error of the off-axis mirror relative to its geometric center (in practice, it is possible that the location of off-axis mirror is correct while it has some rotational error with respect to its geometric center, and we consider these kinds of misalignments rotational misalignments). For on-axis astronomical telescopes, axial and lateral misalignments mainly affect rotationally and non-rotationally symmetric aberrations, respectively (on-axis systems are not affected by rotational misalignments) [9]. In other words, these two kinds of misalignments bear little similarity with each other in on-axis telescopes, and they can hardly couple with each other, making the alignment of on-axis systems comparatively simple and straightforward. However, for off-axis telescopes with an offset pupil, this is not the case. In off-axis telescopes, the rotational symmetry is broken and only plane symmetry is preserved due to pupil decenter. The effects of different kinds of misalignments on the net aberration fields bear some similarities, and they can couple tightly together in practice.

In our previous work, we presented a systematic discussion on the effects of lateral, axial, and rotational misalignments on the net aberration fields in off-axis astronomical telescopes [5–8] based on the framework of nodal aberration theory (NAT) [10–14]. We analytically expressed the aberration fields of off-axis systems with each kind of misalignment, and pointed out and explained the new aberration field characteristics induced by each kind of misalignment in off-axis systems compared to those in on-axis ones [15,16]. Some valuable insights and theoretical guidance was also provided based on the knowledge of misalignment-induced aberration fields. However, in this previous research, the effects of different kinds of misalignments are discussed in isolation, while in practice different kinds of misalignments exist at the same time and the effects of them couple tightly together. The aberration interactions between different kinds of misalignments require further study for better understanding.

In this paper, we present an in-depth and systematic discussion on the aberrational interactions between axial and lateral misalignments in off-axis two-mirror astronomical telescopes. Rotational misalignments can be converted to a special kind of lateral misalignment (the underlying reason being that pupil-offset off-axis systems can generally be seen as an offset portion of a rotationally symmetric on-axis system), and we no longer consider it [8]. We first derive the aberration function of off-axis two-mirror astronomical telescopes with these two kinds of misalignments under certain approximations. Then we discuss the astigmatic and coma aberration-field characteristics in the presence of these two kinds of misalignments. Importantly, we show that a node will arise in the field of view under certain conditions, which is very different from the case in which only one kind of misalignment exists. We further deeply discuss the mutual compensation and separation of these two kinds of misalignments. Most of this work can be extended to other kind of pupil-offset off-axis astronomical telescopes, such as off-axis three-mirror anastigmatic (TMA) telescopes.

This paper is organized as follows. In Section 2, we derive the aberration function for off-axis two-mirror astronomical telescopes in the presence of axial and lateral misalignments. In Sections 3 and 4, we discuss the astigmatic and coma aberration field characteristics, respectively, with focus placed on some special conditions in which a node will arise. Section 5 investigates the mutual compensation between the non-rotationally symmetric aberration induced by axial and lateral misalignments. We continue to discuss the problem of compensating one kind of misalignment with another, and further propose an analytic method to decouple axial misalignments from lateral misalignments in Section 6. We summarize and conclude this paper in Section 7.

2. ABERRATION FUNCTION OF OFF-AXIS TWO-MIRROR ASTRONOMICAL TELESCOPES IN THE PRESENCE OF AXIAL AND LATERAL MISALIGNMENTS

The aberration function of the misaligned off-axis two-mirror astronomical telescopes will be derived based on third-order NAT and a system-level pupil coordination transformation [17]. The specific expressions of astigmatism and coma will be obtained, including the contributions of both axial and lateral misalignments.

The sum of the total aberrations of the system can be attributed to all individual surface contributions [18]. The wave aberration function of rotationally symmetric optical systems can be expressed as [13]

$$\begin{aligned} W_{\text{on-axis}}(\vec{H},\vec{\rho}') &= \sum_j \sum_{p=0}^{\infty} \sum_{n=0}^{\infty} \sum_{m=0}^{\infty} (W_{\text{klm}})_j (\vec{H}\cdot\vec{H})^p (\vec{\rho}'\cdot\vec{\rho}')^n (\vec{H}\cdot\vec{\rho}')^m, \\ k &= 2p+m, \quad l = 2m+n, \end{aligned} \tag{1}$$

where $\vec{H}$ is the normalized field vector, $\vec{\rho}\prime$ is the normalized pupil vector of the on-axis system which is normalized by semi-diameter of the on-axis aperture, and $(W_{\text{klm}})_j$ denotes the aberration coefficient for a particular aberration type of surface j.

Conceptually, we consider that an off-axis telescope is obtained by decentering the aperture stop of an on-axis system, while the other elements of the system (supposing the aperture size of the elements are large enough and the aperture stop cannot move outside of them) stay unchanged [17]. Therefore, according to the system-level pupil coordination transformation, the wave-aberration function of pupil-offset off-axis systems can be expressed as

$$\begin{aligned} W_{\text{off-axis}}(\vec{H},\vec{\rho}) = \sum_j \sum_{p=0}^{\infty} \sum_{n=0}^{\infty} \sum_{m=0}^{\infty} (W_{\text{klm}})_j (\vec{H}\cdot\vec{H})^p [(\vec{\rho}+\vec{s}) \\ \cdot (\vec{\rho}+\vec{s})]^n [\vec{H}\cdot(\vec{\rho}+\vec{s})]^m, \end{aligned} \tag{2}$$

where $\vec{\rho}$ is the normalized pupil vector of the off-axis telescope, which is normalized by the semi-diameter of the off-axis aperture, $\vec{s}$ represents the location of the off-axis pupil relative to the on-axis pupil, which is also normalized by the semi-diameter of the off-axis aperture [17]. When only the third-order aberrations of the on-axis system are considered, Eq. (2) can be rewritten as

$$W_{\text{off-axis}}^{\text{3rd}}(\vec{H},\vec{\rho}) = \sum_j W_{040j}[(\vec{\rho}+\vec{s})\cdot(\vec{\rho}+\vec{s})]^2 + \sum_j W_{131j}[\vec{H}\cdot(\vec{\rho}+\vec{s})][(\vec{\rho}+\vec{s})\cdot(\vec{\rho}+\vec{s})] + \sum_j W_{220Mj}(\vec{H}\cdot\vec{H})[(\vec{\rho}+\vec{s})\cdot(\vec{\rho}+\vec{s})] + \frac{1}{2}\sum_j W_{222j}[\vec{H}^2\cdot(\vec{\rho}+\vec{s})^2] + \sum_j W_{311j}(\vec{H}\cdot\vec{H})[\vec{H}\cdot(\vec{\rho}+\vec{s})], \quad (3)$$

where $W_{220M} = W_{220} + \frac{1}{2}W_{222}$. Here, the subscript M for W_{220} means that the astigmatic aberration is measured with reference to the medial focal surface.

To describe the effects of lateral misalignments, Buchroder introduced a new normalized field vector, $\vec{H}_{Aj}$, to describe the effective field height, which can be expressed as $\vec{H}_{Aj} = \vec{H} - \vec{\sigma}_j$. Here, $\vec{\sigma}_j$ represents the position of the shifted aberration field center for the jth individual surface, which is directly related to the lateral misalignment parameters of the optical system [14]. On the other hand, axial misalignments mainly cause the spherical aberration coefficient W_{040} to change. The field of view (FOV) of off-axis two-mirror astronomical telescopes is usually very small. Therefore, the change of W_{131}, W_{222}, and W_{220} caused by the axial misalignments are higher-order small quantities relative to the change of W_{040} and ΔW_{040d}, and they can be neglected. Therefore, in the presence of lateral and axial misalignments, the wave aberration function of off-axis two-mirror astronomical telescopes can be expressed as

$$W_{\text{off-axis}}^{\text{3rd}}(\vec{H},\vec{\rho}) = \sum_j (W_{040oj}+\Delta W_{040dj})[(\vec{\rho}+\vec{s})\cdot(\vec{\rho}+\vec{s})]^2 + \sum_j W_{131j}[(\vec{H}-\vec{\sigma}_j)\cdot(\vec{\rho}+\vec{s})][(\vec{\rho}+\vec{s})\cdot(\vec{\rho}+\vec{s})] + \sum_j W_{220Mj}[(\vec{H}-\vec{\sigma}_j)\cdot(\vec{H}-\vec{\sigma}_j)][(\vec{\rho}+\vec{s})\cdot(\vec{\rho}+\vec{s})] + \frac{1}{2}\sum_j W_{222j}[(\vec{H}-\vec{\sigma}_j)^2\cdot(\vec{\rho}+\vec{s})^2] + \sum_j W_{311j}[(\vec{H}-\vec{\sigma}_j)\cdot(\vec{H}-\vec{\sigma}_j)][(\vec{H}-\vec{\sigma}_j)\cdot(\vec{\rho}+\vec{s})], \quad (4)$$

where W_{040oj} and ΔW_{040dj} are the initial spherical aberration coefficient of surface j and the change of spherical aberration coefficient, respectively, caused by axial misalignments.

In two-mirror astronomical telescopes, W_{040} is mainly dependent on the distance between primary mirror (PM) and SM, d. Supposing the aperture stop is located at PM, the relationships between W_{040} and the structural parameters of the system are presented as follows [19,20]:

$$\begin{cases} W_{040\text{PM\_sph}} = \frac{D^4 m^3}{512(f'_{\text{SYS}})^3} \\ W_{040\text{PM\_asph}} = \frac{k_{\text{PM}} D^4 m^3}{512(f'_{\text{SYS}})^3} \\ W_{040\text{SM\_sph}} = \frac{D^4 (m+1)^2 (1-m) r}{512(f'_{\text{SYS}})^3}, \\ W_{040\text{SM\_asph}} = \frac{k_{\text{SM}} D^4 (1-m)^3 r}{512(f'_{\text{SYS}})^3} \end{cases} \quad (5)$$

where D is the entrance pupil diameter of the telescope, k_{PM} is the conic constant of the primary mirror, k_{SM} is the conic constant of the SM, $\gamma = \frac{y_{\text{SM}}}{y_{\text{PM}}}$ is the axial obstruction of the system, $m \equiv -\frac{f'_{\text{SYS}}}{f'_{\text{PM}}}$ is the SM magnification, y_{PM} and y_{SM} respectively denote the marginal-ray height on PM and SM, $f'_{\text{SYS}} = \frac{f'_{\text{PM}} f'_{\text{SM}}}{f'_{\text{PM}} - f'_{\text{SM}} - d}$ corresponds to the system focal length, and f'_{PM} and f'_{SM} denote the PM and SM focal length, respectively.

The relationship between W_{040} and d is expressed by system structural parameters as follows (ignoring the higher-order small quantities):

$$W_{040} = W_{040\text{PM\_sph}} + W_{040\text{PM\_asph}} + W_{040\text{SM\_sph}} + W_{040\text{SM\_asph}} = -\frac{D^4}{512 f'^3_{\text{PM}}}\cdot(1+k_{\text{PM}}) + \frac{D^4\gamma}{512}\cdot\frac{-d^3 + (3f'_{\text{PM}} - 4f'_{\text{SM}})d^2 + (8f'_{\text{PM}}f'_{\text{SM}} - 4f'^2_{\text{SM}} - 3f'^2_{\text{PM}})d}{f'^3_{\text{PM}} f'^3_{\text{SM}}} + \frac{D^4\gamma}{512}\cdot\frac{(f'^3_{\text{PM}} - 4f'^2_{\text{PM}}f'_{\text{SM}} + 4f'_{\text{PM}}f'^2_{\text{SM}})}{f'^3_{\text{PM}} f'^3_{\text{SM}}} + \frac{D^4\gamma}{512}\cdot k_{\text{SM}}\frac{-d^3 + 3f'_{\text{PM}}d^2 - 3f'^2_{\text{PM}}d + f'^3_{\text{PM}}}{f'^3_{\text{PM}} f'^3_{\text{SM}}}. \quad (6)$$

By simplifying Eq. (6), we can obtain

$$\Delta W_{040d} = k_{W040d}\cdot\Delta d \quad (7)$$

with

$$k_{W040d} = \frac{D^4\gamma}{512}\cdot\frac{-3d^2 + 2(3f'_{\text{PM}} - 4f'_{\text{SM}})d + (8f'_{\text{PM}}f'_{\text{SM}} - 4f'^2_{\text{SM}} - 3f'^2_{\text{PM}})}{f'^3_{\text{PM}} f'^3_{\text{SM}}} + \frac{D^4\gamma}{512}\cdot k_{\text{SM}}\frac{-3d^2 + 6f'_{\text{PM}}d - 3f'^2_{\text{PM}}}{f'^3_{\text{PM}} f'^3_{\text{SM}}}, \quad (8)$$

where ΔW_{040d} is the net change of W_{040} induced by the change in the distance between PM and SM, Δd. Here, we only consider the first-order term of Δd and neglect those higher-order ones.

On the other hand, the aberration field decenter vectors in the presence of SM misalignments can be expressed as [14]

$$\begin{cases} \vec{\sigma}^{\text{sph}}_{\text{SM}} = \frac{1}{\bar{u}_{\text{PM}}(1+c_{\text{SM}}d)}\begin{pmatrix} \text{BDE}_{\text{SM}} - c_{\text{SM}}\text{XDE}_{\text{SM}} \\ -\text{ADE}_{\text{SM}} - c_{\text{SM}}\text{YDE}_{\text{SM}} \end{pmatrix} \\ \vec{\sigma}^{\text{asph}}_{\text{SM}} = -\frac{1}{d\bar{u}_{\text{PM}}}\begin{pmatrix} \text{XDE}_{\text{SM}} \\ \text{YDE}_{\text{SM}} \end{pmatrix} \end{cases}, \quad (9)$$

where $\vec{\sigma}_{SM}^{sph}$ and $\vec{\sigma}_{SM}^{asph}$ represent the aberration field decenter vectors associated with the spherical base curve and aspheric departure of SM, respectively, XDE_{SM} and YDE_{SM} are the vertex decenters of the SM in the $x-z$ and $y-z$ planes, respectively; ADE_{SM} and BDE_{SM} are the SM tip-tilts in the $x-z$ and $y-z$ planes, respectively; $\bar{u}_{PM}$ is the angle of the chief ray with respect to the optical axis ray, and c_{SM} represents the curvature of the SM.

Consequently, the vector form of wave aberration expansion for the off-axis two-mirror astronomical telescopes with axial and lateral misalignments can be modified as

$$W_{\text{off-axis}} = \begin{bmatrix} \frac{1}{2}\sum_j W_{222j}(\vec{H}^2 - 2\vec{H}\vec{\sigma}_j + \vec{\sigma}_j^2) \\ +2\sum_j (W_{040oj} + \Delta W_{040dj})\vec{s}^2 \\ +\sum_j W_{131j}(\vec{H} - \vec{\sigma}_j)\vec{s} \end{bmatrix} \cdot \vec{\rho}^2 \cdots \text{Astigmatism}$$
$$+ \begin{bmatrix} \sum_j W_{131j}(\vec{H} - \vec{\sigma}_j) \\ +4\sum_j (W_{040oj} + \Delta W_{040dj})\vec{s} \end{bmatrix} \cdot \vec{\rho}(\vec{\rho}\cdot\vec{\rho}) \cdots \text{Coma}$$
$$+ \begin{bmatrix} \sum_j 4(W_{040oj} + \Delta W_{040dj})(\vec{s}\cdot\vec{s}) \\ +2\sum_j W_{131j}(-\vec{\sigma}_j\cdot\vec{s}) \\ +\sum_j W_{220Mj}(\vec{\sigma}_j\cdot\vec{\sigma}_j) \\ +W_{220M}(\vec{H}\cdot\vec{H}) \\ +2W_{131}(\vec{s}\cdot\vec{H}) \\ 2\sum_j W_{220Mj}(-\vec{\sigma}_j\cdot\vec{H}) \end{bmatrix} \cdot (\vec{\rho}\cdot\vec{\rho}) \cdots \text{Defocus}$$
$$+ \text{else}, \tag{10}$$

where we mainly consider the dominant aberrations of the system, i.e., astigmatism, coma, and defocus aberration. This derivation process is similar to that presented in the Appendix of Ref. [7], apart from the fact that W_{040j} should be rewritten as $W_{040j} = W_{040oj} + \Delta W_{040dj}$. It can be seen from Eq. (10) that all three kinds of the dominant aberrations include both the contribution of axial and lateral misalignments.

3. ASTIGMATIC ABERRATION FIELDS IN THE PRESENCE OF AXIAL AND LATERAL MISALIGNMENTS

From this section, we will begin to present an in-depth discussion on the astigmatic and coma aberration fields in the presence of axial and lateral misalignments in off-axis two-mirror astronomical telescopes. Meanwhile, the focus will be placed on the special cases in which a node will arise in the field of view.

A. General Astigmatic Aberration Field Characteristics in the Presence of Axial and Lateral Misalignments

It can be seen from Eq. (10) that the astigmatic aberration field in the presence of both axial and lateral misalignments can be expressed as

$$W_{ast} = \left\{\frac{1}{2}W_{222}\cdot\vec{H}^2 + (W_{131}\vec{s} - \vec{A}_{222})\vec{H} + [(2\Delta W_{040d} + 2W_{040o})\vec{s}^2 - \vec{A}_{131}\vec{s}]\right\}\cdot\vec{\rho}^2, \tag{11}$$

where $\vec{A}_{222} = \sum_j W_{222j}\vec{\sigma}_j$, $\vec{A}_{131} = \sum_j W_{131j}\vec{\sigma}_j$, $\vec{B}_{222} = \sum_j W_{222j}\vec{\sigma}_j^2$. W_{222}, W_{131}, and W_{040o} represent the sums of astigmatic, coma, and initial spherical aberration coefficients, respectively, for all of the individual surfaces. $\vec{B}_{222}$ is a high-order small amount which can be neglected. Therefore, the net astigmatic aberration field induced by axial and lateral misalignments can be simplified as

$$\Delta W_{ast} = [\vec{A}_{222}\cdot\vec{H} + (2\Delta W_{040d}\vec{s}^2 - \vec{A}_{131}\vec{s})]\cdot\vec{\rho}^2. \tag{12}$$

We can see that the net astigmatic aberration field mainly includes a field-linear component and a field-constant component. Considering that off-axis two-mirror astronomical telescopes usually have a small field view, the magnitude of the field-linear component is comparatively small. In other words, it is the field-constant component that mainly determines the astigmatic aberration field, which contains the contributions of both axial and lateral misalignments.

New Solar Telescope (NST) will be used to demonstrate the astigmatic aberration field characteristics just presented. The specific optical prescription and layout of this telescope are presented in Appendix C of [6]. Note that for this off-axis telescope, the pupil decentration vector is given by $\vec{s} = [0, -2.3]^T$, and $\vec{s}$ is the normalized value that corresponds to an offset of 1840 mm of the pupil with a radius of 800 mm $\left(\vec{s} = [0, -\frac{2640-800}{800}]^T\right)$. The full field displays (FFDs) for astigmatism (Z5/Z6) over a $\pm 0.03°$ field of view in the presence of different kinds of misalignments are shown in Fig. 1. Here, we use the PM as the reference. The specific lateral misalignment parameters of the SM are $XDE_{SM} = -0.0200$ mm, $YDE_{SM} = -0.0300$ mm, $ADE_{SM} = 0.0050°$, and $BDE_{SM} = -0.0080°$, and the axial misalignment of the SM is $ZDE_{SM} = -0.1100$ mm. Here, ZDE_{SM} is essentially the same as Δd, for the misalignments of SM in the z direction (ZDE_{SM}) cause change in the despace between PM and SM (Δd). We can recognize that the total aberration contribution of axial and lateral misalignments is the vector superposition of the individual aberration contributions of the two kinds of misalignments, which is consistent with Eq. (12). This indicates that there is a strong coupling relationship between the effects of lateral and axial misalignments.

B. Nodal Properties of Astigmatic Aberration Field in the Presence of Axial and Lateral Misalignments

In general, no node exists in the field of view in the presence of individual axial or lateral misalignments (except that the magnitudes of misalignments are particularly small) [5–7]. However, in the presence of both axial and lateral misalignments, this is not the case. Due to the aberrational interactions between these two kinds of misalignments, a node will arise in the field of view under certain conditions, even if the magnitudes of misalignments are very large (e.g., the misalignments of the SM go beyond its tolerance range).

Equation (11) can be written as

$$W_{ast} = \left\{\frac{1}{2}W_{222}\left(\vec{H} - \frac{\vec{A}_{222} - W_{131}\vec{s}}{W_{222}}\right)^2 - \frac{1}{2}\frac{(\vec{A}_{222} - W_{131}\vec{s})^2}{W_{222}} + [(2\Delta W_{040d} + 2W_{040o})\vec{s}^2 - \vec{A}_{131}\vec{s}]\right\} \cdot \vec{\rho}^2. \quad (13)$$

The position of the astigmatism node in the field of view can be given by

$$\vec{H} = \frac{\vec{A}_{222} - W_{131}\vec{s}}{W_{222}} \pm \sqrt{\frac{(\vec{A}_{222} - W_{131}\vec{s})^2}{W_{222}^2} - \frac{2[(2\Delta W_{040d} + 2W_{040o})\vec{s}^2 - \vec{A}_{131}\vec{s}]}{W_{222}}}. \quad (14)$$

For the special case of $[(2\Delta W_{040d} + 2W_{040o})\vec{s}^2 - \vec{A}_{131}\vec{s}] \approx \vec{0}$, we can obtain the position of the node as

$$\vec{H} = \vec{0} \quad \text{or} \quad \vec{H} = \frac{2(\vec{A}_{222} - W_{131}\vec{s})}{W_{222}}. \quad (15)$$

We can see that in this case there will be a node located near the center of the field of view (the position of the other node may be located outside the field of view). This is one of the important results for the aberrational interactions between axial and lateral misalignments.

A simple example will be utilized to illustrate this special nodal property for astigmatic aberration field in misaligned NST, as shown in Fig. 2, where the lateral misalignments are $XDE_{SM} = -0.0001$ mm, $YDE_{SM} = -0.2000$ mm, $ADE_{SM} = -0.0060°$ and $BDE_{SM} = 0.0002°$, and the axial misalignment of the SM is $ZDE_{SM} = 0.4443$ mm. In this case, the condition of $[(2\Delta W_{040d} + 2W_{040o})\vec{s}^2 - \vec{A}_{131}\vec{s}] \approx \vec{0}$ is satisfied, and a node

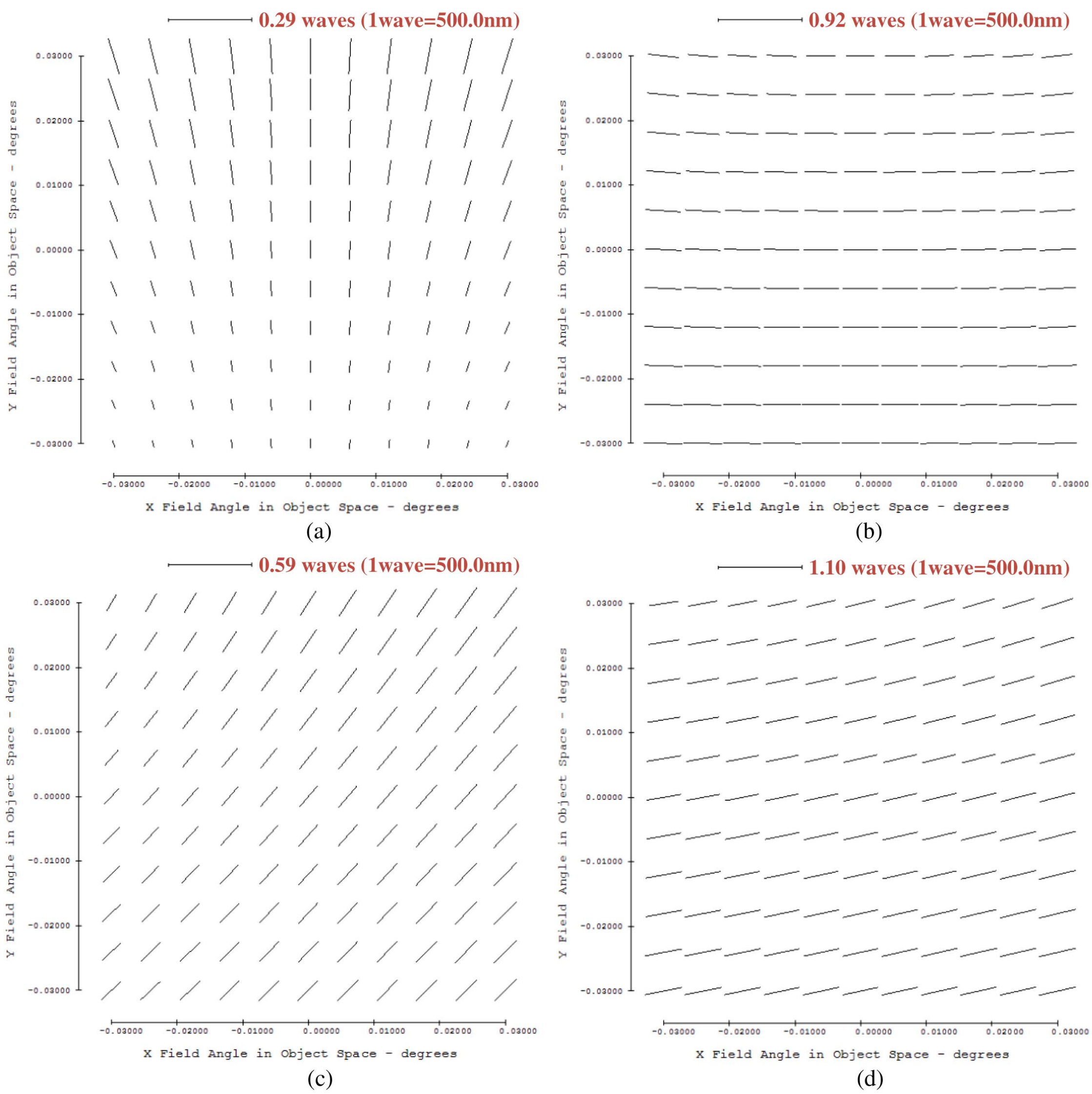

Fig. 1. FFDs for astigmatism (Z5/Z6) in the NST in (a) nominal state and (b), (c, (d) in the presence of different kinds of misalignments. Specifically, (b) and (c) are FFDs for astigmatism in the presence of axial and lateral misalignments, respectively, and (d) is the FFD for astigmatism in the presence of both axial and lateral misalignments. We can recognize that the final astigmatic aberration field is a vector superposition of the individual aberration contributions of the two kinds of misalignments.

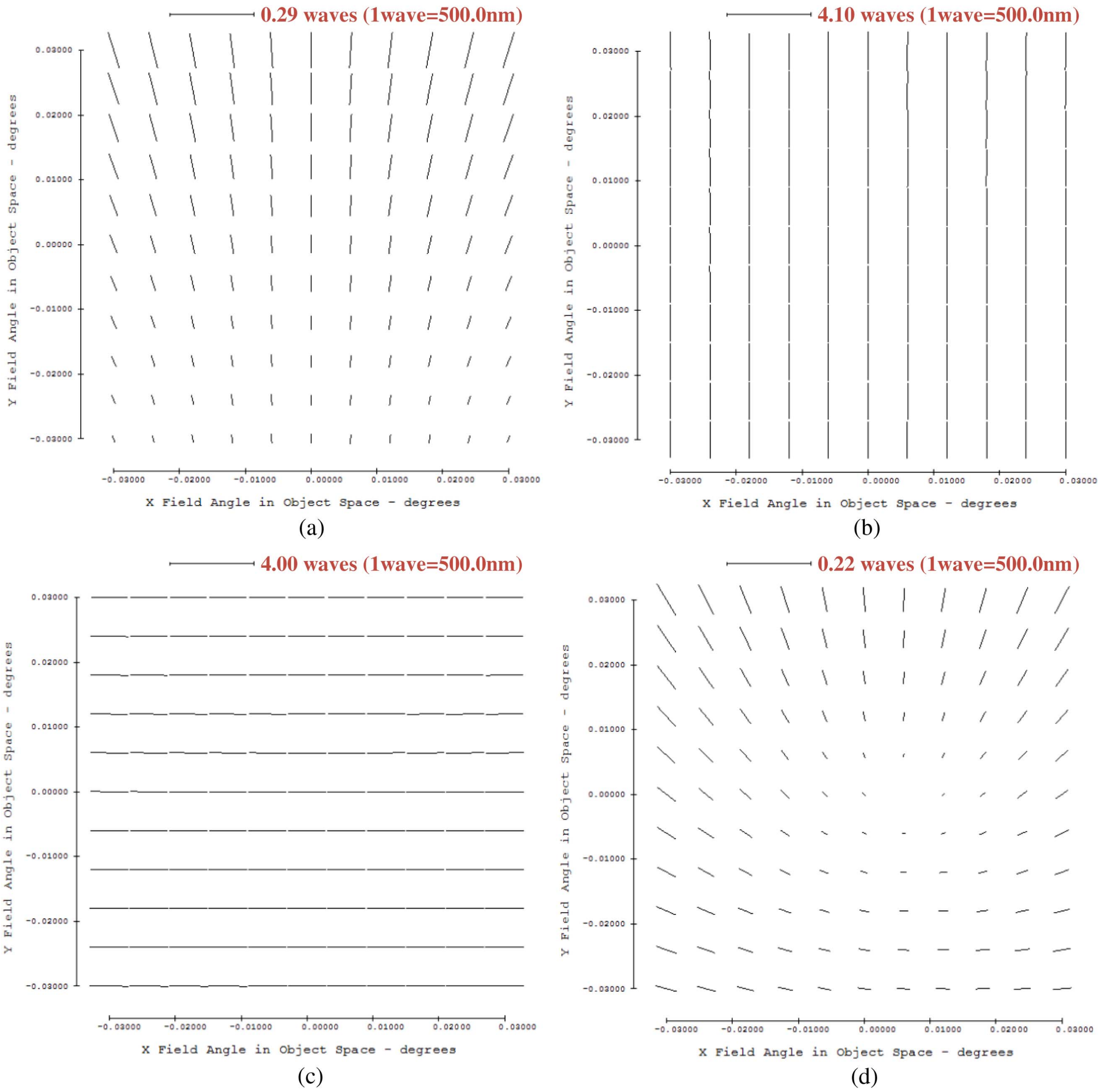

Fig. 2. (a) Nominal astigmatic aberration field. (b) and (c) Astigmatic aberration field in the presence of the designated set of axial and lateral misalignments, respectively (the condition of $[(2\Delta W_{040d} + 2W_{040o})\vec{s}^2 - \vec{A}_{131}\vec{s}] \approx \vec{0}$ is satisfied). (d) Final astigmatic aberration field in the presence of both axial and lateral misalignments. We can see that in the presence of axial or lateral misalignments, a large field-constant astigmatism exists in the field of view, while in the presence of both axial and lateral misalignments, a node can arise in the field of view.

will arise in the field of view, as shown in Fig. 2(d). This indicates that the effects of axial and lateral misalignments can be compensated with each other under certain conditions.

4. COMA ABERRATION FIELDS IN THE PRESENCE OF AXIAL AND LATERAL MISALIGNMENTS

A. General Coma Aberration Field Characteristics in the Presence of Axial and Lateral Misalignments

Referring to Eq. (10), the coma aberration field in off-axis two-mirror astronomical telescopes in the presence of both axial and lateral misalignments can be expressed as

$$W_{\text{coma}} = [W_{131}\vec{H} - \vec{A}_{131} + 4(\Delta W_{040d} + W_{040o})\vec{s}] \cdot \vec{\rho}(\vec{\rho} \cdot \vec{\rho}). \tag{16}$$

The net coma aberration field induced by axial and lateral misalignments (the variation of coma aberration between the nominal and misaligned states) can be simplified as

$$\Delta W_{\text{coma}} = (-\vec{A}_{131} + 4\Delta W_{040d}\vec{s}) \cdot \vec{\rho}(\vec{\rho} \cdot \vec{\rho}), \tag{17}$$

where ΔW_{040d} is related to axial misalignments (ΔW_{040d} is related to Δd) and $\vec{A}_{131}$ is related to lateral misalignments. Specifically, $\vec{A}_{131}$ is related to $\vec{\sigma}_j$ ($\vec{A}_{131} = \sum_j W_{131j}\vec{\sigma}_j$), and $\vec{\sigma}_j$ is related to $\mathrm{XDE_{SM}}, \mathrm{YDE_{SM}}, \mathrm{ADE_{SM}}$, and $\mathrm{BDE_{SM}}$. Equation (17) shows that the magnitude and orientation of the misalignment-induced coma is modulated by the magnitudes of axial and lateral misalignments.

The FFDs for coma (Z7/Z8) over a 0.03° field of view in the presence of different kinds of misalignments are shown in Fig. 3. The specific lateral misalignment parameters of the SM are $\mathrm{XDE_{SM}} = 0.0500$ mm, $\mathrm{YDE_{SM}} = -0.0300$ mm,

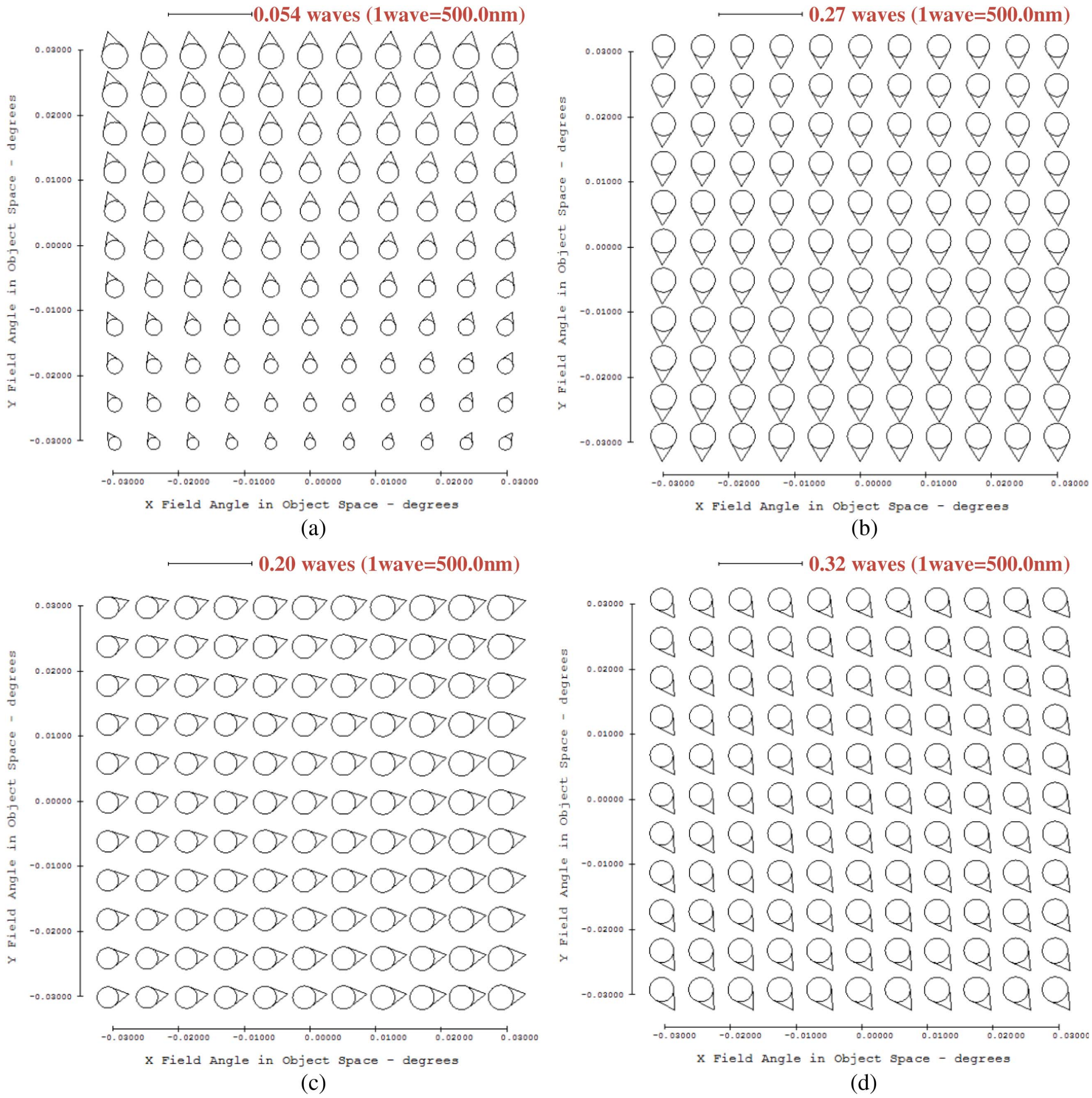

Fig. 3. FFDs for coma (Z7/Z8) in the NST in (a) nominal state and (b)–(d) in the presence of different kinds of misalignments. Specifically, (b) and (c) are FFDs for coma in the presence of axial and lateral misalignments, respectively, and (d) is the FFD for coma in the presence of both axial and lateral misalignments. We can recognize that total coma aberration induced by axial and lateral misalignments is the vector superposition of the individual aberration contributions of the two kinds of misalignments.

$ADE_{SM} = 0.0060°$, and $BDE_{SM} = -0.0030°$, and the axial misalignment of the SM is $ZDE_{SM} = -0.1230$ mm. We can further recognize that the total aberration contribution of axial and lateral misalignments is still the vector superposition of the individual aberration contribution of the two kinds of misalignments, which is consistent with Eq. (17). This fact further indicates that there is a strong coupling relationship between the effects of lateral and axial misalignments.

B. Nodal Properties of Coma Aberration Field in the Presence of Axial and Lateral Misalignments

According to Eq. (16), the position of the coma node in the field of view can be given by

$$\vec{H} = \frac{\vec{A}_{131} - 4(\Delta W_{040d} + W_{040o})\vec{s}}{W_{131}}. \tag{18}$$

We can see that there will be a node in the field of view ($|\vec{H}| < 1$) if the condition of $|\vec{A}_{131} - 4(\Delta W_{040d} + W_{040o})\vec{s}| < |W_{131}|$ is satisfied. If the condition of $\vec{A}_{131} - 4(\Delta W_{040d} + W_{040o})\vec{s} \approx \vec{0}$ is satisfied, this node will move close to the center of the field of view.

Then an example will be utilized to illustrate this special nodal property for coma aberration field in misaligned NST, as shown in Fig. 4, where the specific lateral misalignment parameters are $XDE_{SM} = -0.0100$ mm, $YDE_{SM} = 0.0592$ mm, $ADE_{SM} = 0.0093°$, and $BDE_{SM} = -0.0019°$, and the axial misalignment of the SM is $ZDE_{SM} = -0.1000$ mm. In this case, the condition of $\vec{A}_{131} - 4(\Delta W_{040d} + W_{040o})\vec{s} \approx \vec{0}$ is satisfied, and a node will arise near the field center. This fact further indicates that the effects of axial and lateral misalignments can be compensated with each other under certain conditions. In fact, there is an infinite number

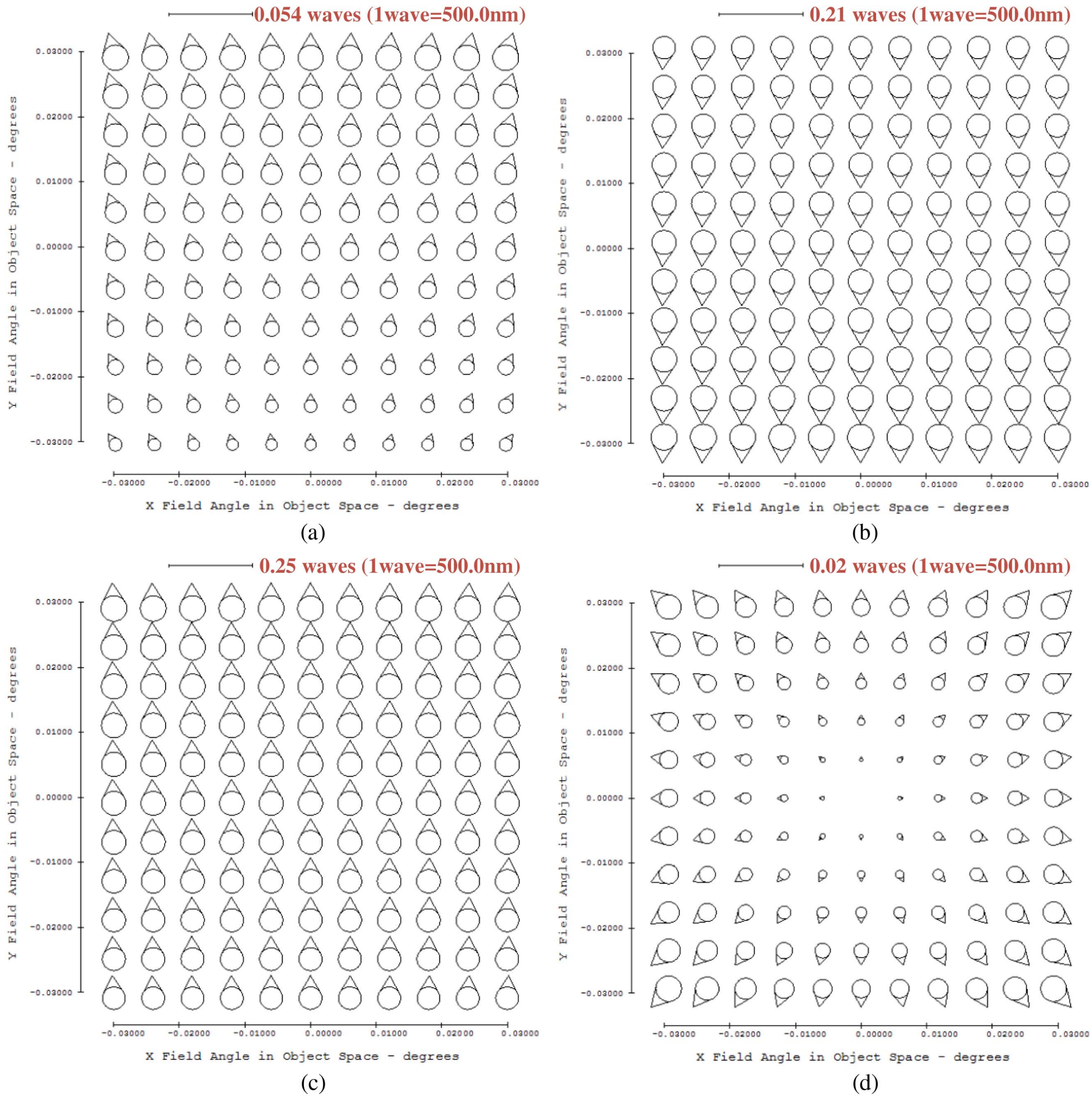

Fig. 4. (a) Nominal coma aberration field. (b) and (c) Coma aberration field in the presence of the designated set of axial and lateral misalignments, respectively (the condition of $\vec{A}_{131} - 4(\Delta W_{040d} + W_{040o})\vec{s} \approx \vec{0}$ is satisfied). (d) Final coma aberration field in the presence of both axial and lateral misalignments. We can see that in the presence of axial or lateral misalignments, a large field-constant coma exists in the field of view, while in the presence of both axial and lateral misalignments, a node can arise in the field of view, similar to the case of the astigmatic aberration field.

of possible combinations of axial and lateral misalignments to fulfill this condition. However, we cannot choose arbitrary lateral misalignment first and then find the axial misalignment which satisfies the condition, as $\vec{A}_{131}$ has components in the x and y axes, while $\vec{s}$ only has component in the y axis. On the other hand, under the condition of $\mathrm{XDE_{SM}} = \mathrm{BDE_{SM}} = 0$, we can choose $\mathrm{YDE_{SM}}$ and $\mathrm{ADE_{SM}}$ randomly. We can further discuss this problem in Section 5.B.

5. MUTUAL COMPENSATION BETWEEN AXIAL AND LATERAL MISALIGNMENTS

In Section 4, we pointed out that under certain conditions, a node will arise in the field of view for both the astigmatic and coma aberration fields. The underlying reason is that the dominant field-constant astigmatism or coma term includes aberration contributions of both axial and lateral misalignments, and they can be compensated by each other under certain conditions. In this section, we will continue to discuss the mutual compensation between axial and lateral misalignments. It will be shown that the astigmatic and coma aberration fields induced by axial misalignments can well be compensated with lateral misalignments, while axial misalignments can only compensate 0° astigmatism and 90° coma induced by lateral misalignments.

A. Mutual Compensation between Axial and Lateral Misalignments for an Astigmatic Aberration Field

Since the field of view of the two-mirror astronomical telescope system is usually small, we here only consider the field-constant astigmatism term and neglect the field-linear term when discussing the aberrational compensation between the two kinds of

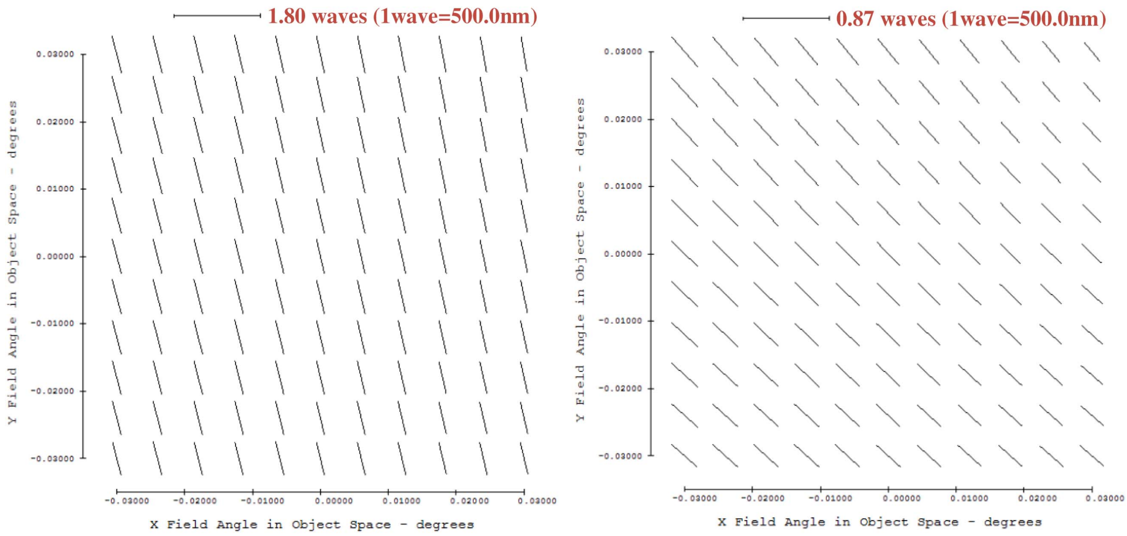

(a) (b)

Fig. 5. FFDs for astigmatism (Z5/Z6) in the presence of (a) lateral misalignments and (b) after compensating the astigmatism induced by lateral misalignments with axial misalignments. We can see that a large 45° astigmatism still exists in the field of view. This fact indicates that it is not proper to compensate for the astigmatism induced by lateral misalignments with axial misalignments, for axial misalignments can only affect 0° astigmatism.

misalignments. According to Eq. (12), the conditions in which the two kinds of misalignments can be compensated by each other for astigmatism can be given by

$$\begin{cases} \Delta C_5 = 0 \\ \Delta C_6 = 0 \end{cases} \Rightarrow \begin{cases} \vec{A}_{131y} = 2k_{W040d}\vec{s}_y \cdot \Delta d \\ A_{131,x} = 0 \end{cases}. \tag{19}$$

Here, we first discuss compensating the astigmatism induced by lateral misalignments by introducing axial misalignments. We can see that only the 0° astigmatism induced by lateral misalignments can be compensated with axial misalignments, for axial misalignments cannot affect 45° astigmatism. After using axial misalignments to compensate for the astigmatism induced by lateral misalignments, a field-constant 45° astigmatism will remain in the field of view.

We take NST as an example to illustrate this compensation process, which is shown in Fig. 5. The specific lateral misalignment parameters of the SM used here are $\mathrm{XDE}_{\mathrm{SM}} = -0.0200$ mm, $\mathrm{YDE}_{\mathrm{SM}} = 0.0800$ mm, $\mathrm{ADE}_{\mathrm{SM}} = -0.0010°$, and $\mathrm{BDE}_{\mathrm{SM}} = 0.0030°$. According to Eq. (19), we can obtain the axial misalignments needed to compensate for the effects of lateral misalignments, and the result is $\Delta d = -0.1565$ mm. We can see that the 0° astigmatism is well compensated by axial misalignments while a large 45° astigmatism still exists in the field of view.

Then, we continue to discuss compensating the astigmatic aberration contribution of axial misalignments with lateral misalignments. To compute the lateral misalignments for compensating axial misalignments, Eq. (19) can be rewritten as

$$\begin{cases} 2k_{W040d}\vec{s}_y\Delta d = (W_{131\mathrm{SM\_sph}}\vec{\sigma}^{\mathrm{sph}}_{\mathrm{SM},y} + W_{131\mathrm{SM\_asph}}\vec{\sigma}^{\mathrm{asph}}_{\mathrm{SM},y}) \\ (W_{131\mathrm{SM\_sph}}\vec{\sigma}^{\mathrm{sph}}_{\mathrm{SM},x} + W_{131\mathrm{SM\_asph}}\vec{\sigma}^{\mathrm{asph}}_{\mathrm{SM},x}) = 0. \end{cases} \tag{20}$$

Substituting Eq. (9) into Eq. (20), we can obtain

$$\begin{cases} \mathrm{YDE}_{\mathrm{SM}} = \dfrac{-2k_{W040d}\Delta d\vec{s}_y(1+c_{\mathrm{SM}}d)\bar{u}_{\mathrm{PM}}d - W_{131\mathrm{SM\_sph}}d\,\mathrm{ADE}_{\mathrm{SM}}}{W_{131\mathrm{SM\_sph}}c_{\mathrm{SM}}d + W_{131\mathrm{SM\_asph}}c_{\mathrm{SM}}d + W_{131\mathrm{SM\_asph}}} \\ \mathrm{XDE}_{\mathrm{SM}} = \mathrm{BDE}_{\mathrm{SM}} = 0. \end{cases} \tag{21}$$

We can see that we only need to change the lateral misalignment parameters located in the $y-z$ plane ($\mathrm{YDE}_{\mathrm{SM}}$ and $\mathrm{ADE}_{\mathrm{SM}}$) when compensating the astigmatism induced by axial misalignments.

To illustrate this compensation process, we assume that the axial misalignment of SM in NST is $\mathrm{ZDE}_{\mathrm{SM}} = -0.2$ mm (the tolerance for SM despace in NST is ± 0.2 mm [21]). Then we use one set of lateral misalignments to compensate for the astigmatism induced by axial misalignments. Here, we only use the decenter parameter of the SM to achieve this goal ($\mathrm{ADE}_{\mathrm{SM}} = 0°$), and we can compute that the compensating parameter is $\mathrm{YDE}_{\mathrm{SM}} = 0.0956$ mm. The astigmatic aberration field before and after introducing lateral misalignments is shown in Figs. 6(a) and 6(b), respectively. We can see that after introducing the set of lateral misalignments just presented, the astigmatic aberration field is nearly corrected to the nominal state.

B. Mutual Compensation between Axial and Lateral Misalignments for a Coma Aberration Field

Referring to Eq. (17), the conditions in which the two kinds of misalignments can be compensated by each other for coma aberration can be given by

$$\begin{cases} \Delta C_7 = 0 \\ \Delta C_8 = 0 \end{cases} \Rightarrow \begin{cases} \vec{A}_{131,x} = 0 \\ 4k_{W040d}\Delta d\vec{s}_y - \vec{A}_{131,y} = 0. \end{cases} \tag{22}$$

We first discuss compensating coma aberration induced by lateral misalignments with axial misalignments. We can see

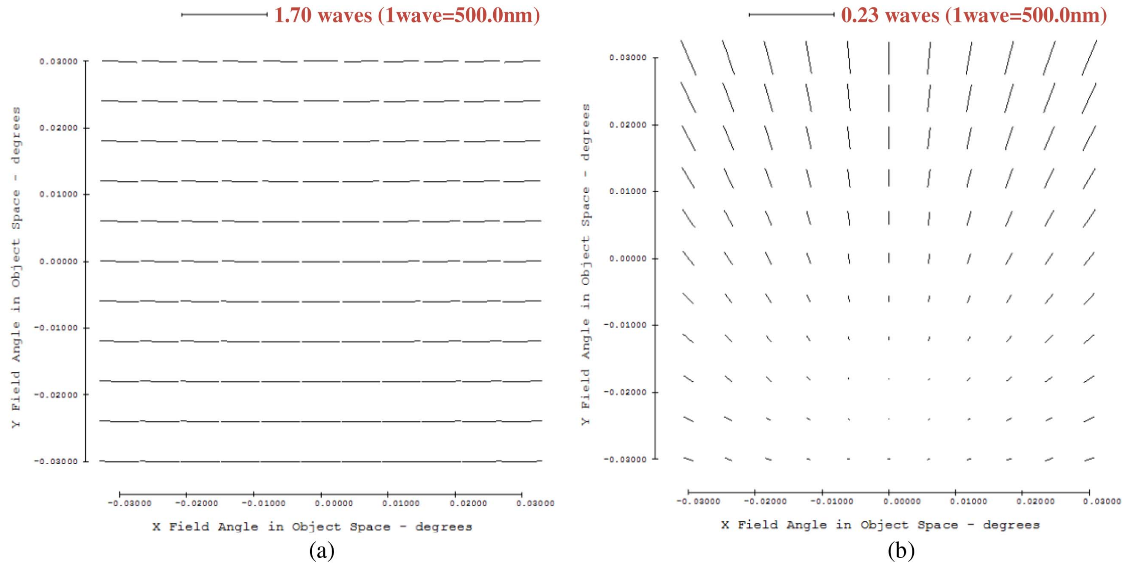

Fig. 6. FFDs for astigmatism (Z5/Z6) in the presence of (a) axial misalignments and (b) after compensating for the effects of axial misalignments with lateral misalignments. We can see that the 0° astigmatism induced by axial misalignments has been compensated for by 0° astigmatism induced by lateral misalignments, and the astigmatism distribution is close to the nominal state.

from Eq. (22) that axial misalignments only affect the 90° coma. In other word, axial misalignments can only compensate for the 90° coma induced by lateral misalignments.

Figure 7 illustrates this compensation process. The specific lateral misalignment parameters of the SM are $\mathrm{XDE_{SM}} = 0.0800$ mm, $\mathrm{YDE_{SM}} = 0.0100$ mm, $\mathrm{ADE_{SM}} = -0.0300°$, and $\mathrm{BDE_{SM}} = 0.0030°$. Then, $4k_{W040d}\Delta d\vec{s}_y - \vec{A}_{131,y} = 0$ is used to calculate the compensating axial misalignment and the result is $\Delta d = 0.1539$ mm. Thus, the axial misalignment of the SM used for aberration compensation is $\mathrm{ZDE_{SM}} = 0.1539$ mm. We can see that the 90° coma is well compensated by axial misalignments, while a 0° coma still exists in the field of view.

Then we continue to discuss compensating the coma aberration contribution of axial misalignments with lateral misalignments. Equation (22) can be rewritten as

$$\begin{cases} W_{131\mathrm{SM\_sph}}\vec{\sigma}^{\mathrm{sph}}_{\mathrm{SM},x} + W_{131\mathrm{SM\_asph}}\vec{\sigma}^{\mathrm{asph}}_{\mathrm{SM},x} = 0 \\ 4k_{W040d}\vec{s}_y\Delta d = (W_{131\mathrm{SM\_sph}}\vec{\sigma}^{\mathrm{sph}}_{\mathrm{SM},y} + W_{131\mathrm{SM\_asph}}\vec{\sigma}^{\mathrm{asph}}_{\mathrm{SM},y}). \end{cases} \tag{23}$$

Substituting Eq. (9) into Eq. (23), we can obtain

$$\begin{cases} \mathrm{XDE_{SM}} = \mathrm{BDE_{SM}} = 0 \\ \mathrm{YDE_{SM}} = \dfrac{-4k_{W040d}\Delta d\vec{s}_y(1+c_{\mathrm{SM}}d_1)\bar{u}_{\mathrm{PM}}d - W_{131\mathrm{SM\_sph}}d\,\mathrm{ADE_{SM}}}{W_{131\mathrm{SM\_sph}}c_{\mathrm{SM}}d + W_{131\mathrm{SM\_asph}}c_{\mathrm{SM}}d + W_{131\mathrm{SM\_asph}}}. \end{cases} \tag{24}$$

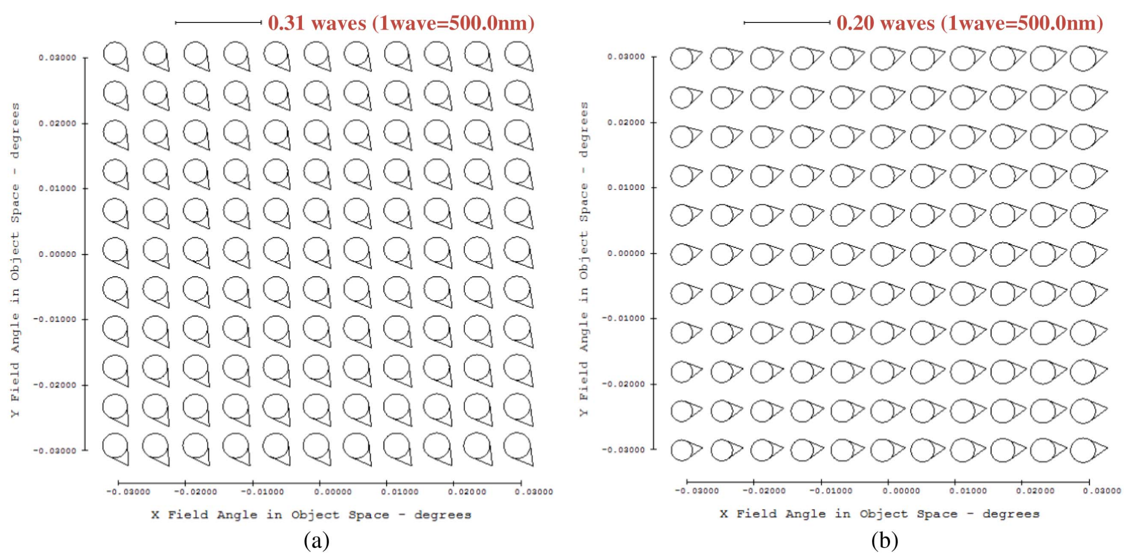

Fig. 7. FFDs for coma (Z7/Z8) in the presence of (a) lateral misalignments and (b) after compensating for the coma induced by lateral misalignments with axial misalignments. We can see that a large 0° coma still exists in the field of view. This fact indicates that it is not proper to compensate for the coma induced by lateral misalignments with axial misalignments, for axial misalignments can affect only 90° coma.

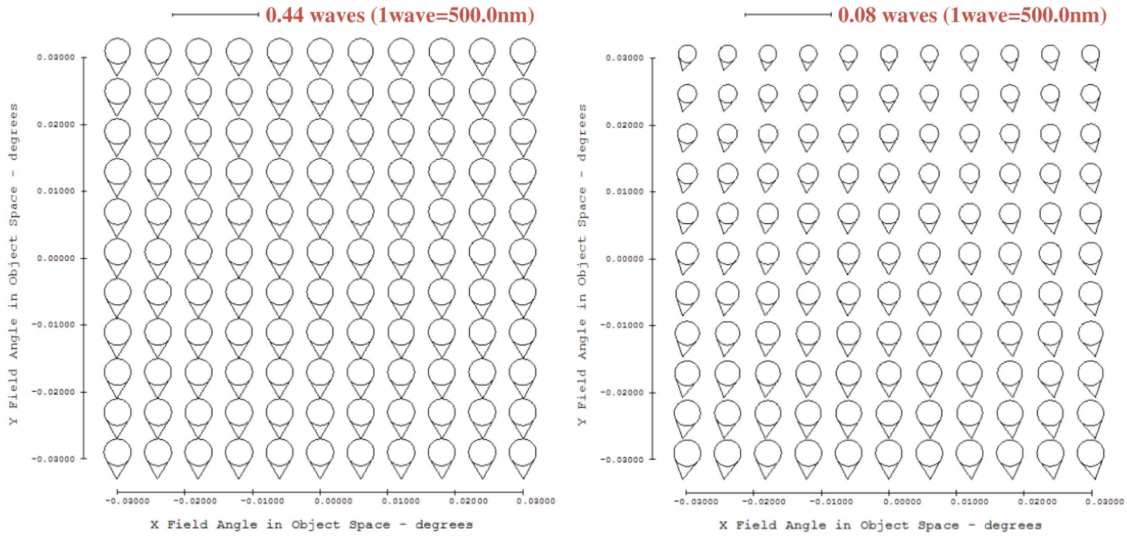

(a) (b)

Fig. 8. FFDs for coma (Z7/Z8) in the presence of (a) axial misalignments and (b) after compensating for the coma induced by axial misalignments with lateral misalignments. We can see that the 90° coma induced by axial misalignments is well compensated by the introduced lateral misalignments, and the coma aberration field is nearly corrected to the nominal state.

We can see that we only need to change the lateral misalignment parameters located in the $y-z$ plane (YDE_{SM} and ADE_{SM}) when compensating the coma aberration induced by axial misalignments (ZDE_{SM} or Δd).

To illustrate this compensation process, we assume that the axial misalignments of SM in NST is also $ZDE_{SM} = -0.2000$ mm. Then we use the decenter parameter of the SM to compensate for the astigmatism induced by axial misalignments, and we can calculate $YDE_{SM} = 0.1911$ mm. The coma aberration field before and after introducing this lateral misalignment are shown in Figs. 8(a) and 8(b), respectively. We can see that the large 90° coma induced by axial misalignments is nearly corrected to the nominal state.

C. Other Discussion

In the two subsections just presented, we demonstrate that the individual astigmatic or coma aberration field induced by axial misalignments can well be compensated with lateral misalignments, while it is not proper to compensate for the effects of lateral misalignments with axial misalignments. In this

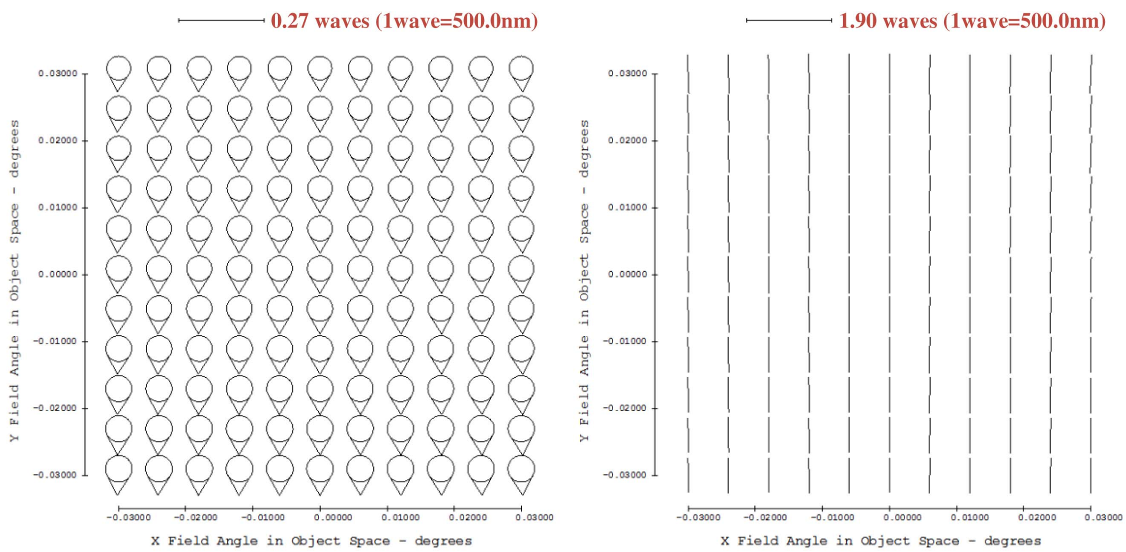

(a) (b)

Fig. 9. (a) FFD for coma aberration field after introducing lateral misalignments to compensate for the astigmatism induced by axial misalignments and (b) FFD for astigmatism after introducing lateral misalignments to compensate for the coma induced by axial misalignments. By referring to Figs. 8(a) and 6(a), we can recognize that when we use lateral misalignments to compensate for astigmatism induced by axial misalignments, the magnitude of the coma will also decrease. However, when we use lateral misalignments to compensate for coma induced by axial misalignments, the magnitude of astigmatism is nearly the same as that before aberration compensation, but the direction is opposite.

subsection, we further present a brief discussion on the case of compensating the effects of axial misalignments with lateral misalignments when astigmatic and coma aberration field are taken into consideration at the same time.

We can recognize that coefficients before the constant $k_{W040d}\Delta d\vec{s}_y(1+c_{\mathrm{SM}}d)\bar{u}_{\mathrm{PM}}d$ in Eqs. (21) and (24) are different in magnitude (but same in sign). This indicates that the astigmatism and coma aberration induced by axial misalignments cannot be compensated for by lateral misalignments at the same time. Considering that astigmatism is more sensitive to misalignments than coma in pupil-offset off-axis systems [5,6], generally we can use lateral misalignments to compensate for astigmatism and neglect the residual coma (the magnitude of coma will also be decreased in this process). Otherwise, if we use lateral misalignments to compensate for the coma induced by axial misalignments, a large astigmatism aberration will still remain in the field of view, the direction of which is opposite to the original astigmatism induced by axial misalignments (the magnitude of the residual astigmatism is nearly the same as that before compensation).

Supposing that the axial misalignment of the SM is also $\mathrm{ZDE}_{\mathrm{SM}} = -0.2000$ mm, the coma aberration field after introducing lateral misalignments to compensate for the astigmatism is shown in Fig. 9(a), and the astigmatic aberration field after introducing lateral misalignments to compensate for the coma is shown in Fig. 9(b). Comparing Fig. 9(a) with Fig. 8(a), we can see that in the process of compensating astigmatic aberration field, the magnitude of the coma will also be reduced. However, comparing Fig. 9(b) with Fig. 6(a), we can see that in the process of compensating coma aberration, the magnitude of the astigmatic aberration field will increase in the opposite direction.

We should also note that if the magnitudes of axial misalignments are comparatively large (e.g., going beyond the tolerance for misalignments of SM), a large coma will remain in the field of view, compared with the nominal state, after using lateral misalignments to compensate for astigmatism induced by axial misalignments. In practice, if we find there exists some coma in the field while little astigmatism exists in an off-axis telescope, one of the possible reasons is that there exist both axial and lateral misalignments in the system and they are in a compensating state for astigmatism.

6. SEPARATION OF THE EFFECTS OF AXIAL AND LATERAL MISALIGNMENTS

In the discussions just presented, we show that both the astigmatism and coma induced by axial misalignments can be compensated for by introducing lateral misalignments to a large extent. On the other hand, we also point out that if the magnitudes of axial misalignments are very large, a large coma will remain in the field of view. In this section, we will further show that when compensating the astigmatism or coma using one kind of misalignment, the defocus aberration will consistently become larger.

Therefore, in practice, it is better to decouple the effects of axial and lateral misalignments. In this section, an analytic method will be proposed to separate these two kinds of misalignments when wavefront measurement at only one field point is available.

A. Analysis of the Defocus Aberration in the Process of Aberration Compensation

When discussing the mutual compensation between axial and lateral misalignments, we only consider the non-rotationally symmetric aberrations (i.e., astigmatism and coma). In effect, after compensation, the magnitude of the defocus aberration will become larger compared with that in the presence of one kind of misalignment.

Here, we take the case of compensating for the astigmatism induced by axial misalignments with lateral misalignments as an example to illustrate this problem, as shown in Fig. 10. The specific axial misalignment parameter is $\Delta d = -0.2000$ mm, and the compensating lateral misalignment parameters are $\mathrm{ADE}_{\mathrm{SM}} = 0.0000°$ and $\mathrm{YDE}_{\mathrm{SM}} = 0.0956$ mm. We can see that after compensating for the astigmatism induced by axial misalignments with lateral misalignments, the defocus aberration will become larger.

Here, we will give a brief explanation for this result. In the presence of axial and lateral misalignments, we can obtain

$$\Delta W_{\mathrm{defocus}} = \Delta W_{\mathrm{defocus}}^{(\mathrm{axial})} + \Delta W_{\mathrm{defocus}}^{(\mathrm{lateral})}, \tag{25}$$

where defocus aberration induced by axial and lateral misalignments can be expressed as

$$\begin{cases} \Delta W_{\mathrm{defocus}}^{(\mathrm{axial})} = \frac{\varepsilon_Z}{8(F^\#)^2} + k_{W040d}\Delta d\vec{s}_y^{\,2}, \\ \Delta W_{\mathrm{defocus}}^{(\mathrm{lateral})} = \left(W_{131,\mathrm{sph}}\frac{\mathrm{ADE}_{\mathrm{SM}}+c_{\mathrm{SM}}\mathrm{YDE}_{\mathrm{SM}}}{(1+c_{\mathrm{SM}}d)\bar{u}_{\mathrm{PM}}} + W_{131,\mathrm{asph}}\frac{\mathrm{YDE}_{\mathrm{SM}}}{d\bar{u}_{\mathrm{PM}}}\right)\vec{s}_y. \end{cases} \tag{26}$$

Here, $F^\#$ is F number and ε_Z represents the shift of the focal plane induced by the axial misalignments; we neglect the field-dependent terms and the quadratic small quantities in this equation. The specific expressions of $F^\#$ and ε_Z are given by

$$\begin{cases} F^\# = \frac{f'_{\mathrm{NEW}}}{D}, \\ \varepsilon_Z = d_2 - l'_F, \end{cases} \tag{27}$$

where

$$\begin{cases} f'_{\mathrm{NEW}} = \frac{f'_{\mathrm{PM}}f'_{\mathrm{SM}}}{f'_{\mathrm{PM}}-f'_{\mathrm{SM}}-(d+\Delta d)}, \\ l'_F \approx f'_{\mathrm{NEW}}\cdot\left(1-\frac{d}{f'_{\mathrm{PM}}}\right). \end{cases} \tag{28}$$

Here, f'_{NEW} is focal length of the system in the presence of axial misalignments; d_2 is the distance from SM to image plane, which is a positive number; and l'_F is the distance from the SM to the focus.

In general, $\left|\frac{\varepsilon_Z}{8(F^\#)^2}\right| \gg |k_{W040d}\Delta d\vec{s}_y^{\,2}|$, and we can only consider $\frac{\varepsilon_Z}{8(F^\#)^2}$ for defocus aberration induced by axial misalignments. Here, we first assume that $\Delta d < 0$, and then we know that the distance between SM and PM becomes larger (d is a negative number). Then the focus will be shifted to the direction of SM. Supposing the position of the image plane stays unchanged, ε_Z is a positive number. In other words, $\Delta W_{\mathrm{defocus}}^{(\mathrm{axial})}$ is a positive number when $\Delta d < 0$. At the same time, we find that the sign of $\frac{\varepsilon_Z}{8(F^\#)^2}$ and $k_{W040d}\Delta d\vec{s}_y^{\,2}$ are opposite, for $k_{W040d} > 0$ in NST.

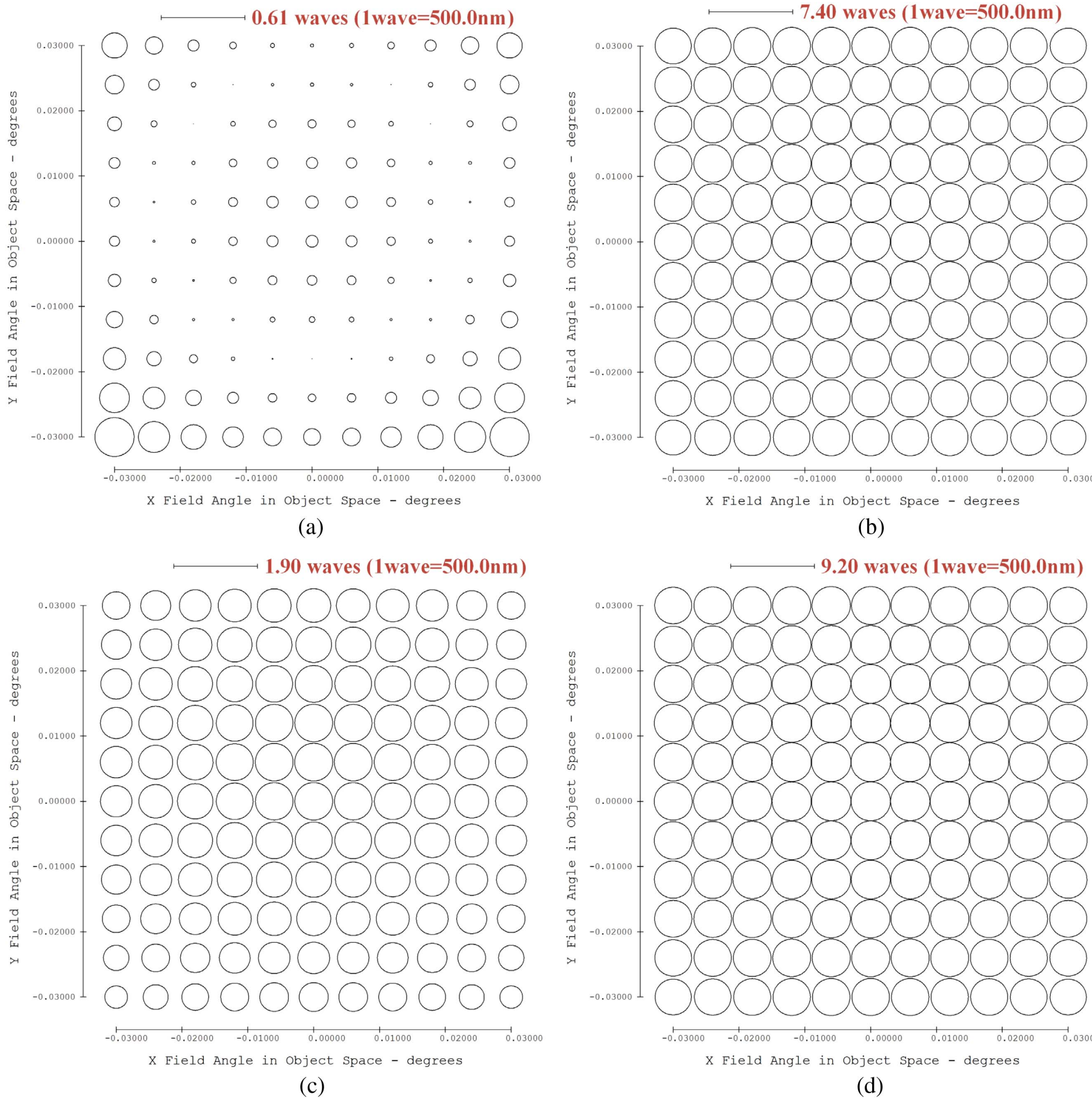

Fig. 10. FFDs for defocus aberration (Z4) in the NST in different cases. (a) shows defocus aberration in the nominal state, (b) shows the defocus aberration in the presence of axial misalignments, (c) shows the defocus aberration in the presence of lateral misalignments, and (d) shows defocus aberration in the presence of axial and lateral misalignments, where lateral misalignments compensate the astigmatic aberration field induced by axial misalignments. We can see that when using lateral misalignments to compensate for astigmatism, the defocus aberration will become larger.

As can be known from the third section, when we discuss the mutual compensation between axial and lateral misalignments about astigmatism, we must satisfy

$$2k_{W040d}\Delta d = -\left[\frac{W_{131\text{SM\_sph}}\left(\frac{\text{ADE}_{\text{SM}}+c_{\text{SM}}\text{YDE}_{\text{SM}}}{(1+c_{\text{SM}}d)\bar{u}_{\text{PM}}}\right)+W_{131\text{SM\_asph}}\left(\frac{\text{YDE}_{\text{SM}}}{d\bar{u}_{\text{PM}}}\right)}{\vec{s}_y}\right]. \quad \textbf{(29)}$$

The sign of $(W_{131,\text{sph}}\frac{\text{ADE}_{\text{SM}}+c_{\text{SM}}\text{YDE}_{\text{SM}}}{(1+c_{\text{SM}}d)\bar{u}_{\text{PM}}}+W_{131,\text{asph}}\frac{\text{YDE}_{\text{SM}}}{d\bar{u}_{\text{PM}}})\vec{s}_y$ is contrary to that of $k_{W040d}\Delta d\vec{s}_y^{\,2}$. This suggests that the signs of defocus introduced by the axial and lateral misalignments are identical, and the total defocus is equal to the sum of defocus caused by the two kinds of misalignment. At the same time, this superposition relationship still exists when $\Delta d > 0$. This conclusion is applicable not only to NST, but also to other off-axis two-mirror astronomical telescopes.

B. Separation of the Effects of Lateral and Axial Misalignments

As just presented, the astigmatic and coma aberration induced by axial and lateral misalignments can be expressed as

$$\begin{cases} \Delta W_{\text{ast}} = (-\vec{A}_{131}\vec{s}+2\Delta W_{040d}\vec{s}^{\,2})\cdot\vec{\rho}^{\,2} \\ \Delta W_{\text{coma}} = (-\vec{A}_{131}+4\Delta W_{040d}\vec{s})\cdot\vec{\rho}(\vec{\rho}\cdot\vec{\rho}) \end{cases}, \quad \textbf{(30)}$$

where we neglect the field-dependent terms.

Table 1. Three Different Misalignment Ranges in Monte Carlo Simulation

	XDE_{SM}/YDE_{SM}[a]	ADE_{SM}/BDE_{SM}[b]	Δd[a]	Measurement Error
Case 1	[−0.05, 0.05]	[−0.005, 0.005]	[−0.1, 0.1]	/
Case 2	[−0.1, 0.1]	[−0.01, 0.01]	[−0.2, 0.2]	/
Case 3	[−0.1, 0.1]	[−0.01, 0.01]	[−0.2, 0.2]	3%

[a] XDE_{SM}, YDE_{SM} and Δd are measured in millimeters.
[b] ADE_{SM}, BDE_{SM} are measured in degrees.

At the same time, wave aberration can also be described as a sum of the weighted Zernike polynomial. The polynomial can be expressed as

$$\begin{cases} \Delta W_{ast,x} = \Delta C_5 \cdot \rho^2 \cdot \cos(2\theta) \\ \Delta W_{ast,y} = \Delta C_6 \cdot \rho^2 \cdot \mathrm{sins}(2\theta) \\ \Delta W_{coma,x} = \Delta C_7 \cdot (3\rho^2 - 2) \cdot \rho \cdot \cos(\theta) \\ \Delta W_{coma,y} = \Delta C_8 \cdot (3\rho^2 - 2) \cdot \rho \cdot \mathrm{sins}(\theta) \end{cases}, \quad (31)$$

where C_i is the corresponding Fringe Zernike coefficient, and ρ and θ are the magnitude and azimuth angle of $\vec{\rho}$, respectively.

Referring to the relationship between Seidel aberration coefficients and Fringe Zernike aberration coefficients [22], Eq. (30) can be rewritten as

$$\begin{bmatrix} 0 & \vec{h}_y & -2\vec{s}_y^{\,2} \\ -\vec{s}_y & 0 & 0 \\ -\frac{1}{3} & 0 & 0 \\ 0 & -\frac{1}{3} & \frac{4}{3}\vec{s}_y \end{bmatrix} \begin{bmatrix} \vec{A}_{131,x} \\ \vec{A}_{131,y} \\ \Delta W_{040d} \end{bmatrix} = \begin{bmatrix} \Delta C_5 \\ \Delta C_6 \\ \Delta C_7 \\ \Delta C_8 \end{bmatrix}. \quad (32)$$

Then, $[\vec{A}_{222,x} \quad \vec{A}_{222,y} \quad \Delta W_{040d}]^T$ can be calculated with the equation

$$[\vec{A}_{222,x} \quad \vec{A}_{222,y} \quad \Delta W_{040d}]^T = (\mathbf{A}_i^T \mathbf{A}_i)^{-1} \mathbf{A}_i^T \Delta C, \quad (33)$$

where $\Delta C \equiv [\Delta C_5 \, \Delta C_6 \, \Delta C_7 \, \Delta C_8]^T$, the superscript T represents the matrix transpose operation, and the superscript -1 represents the matrix inversion operation.

After solving ΔW_{040d}, we can calculate the axial misalignment of SM according to $\Delta d = \frac{\Delta W_{040d}}{k_{W040d}}$. Then the aberrations induced by the axial misalignment of the SM can be removed by correcting this kind of misalignment. On the other hand, the remaining lateral misalignments can be solved according to the current analytic model [6,23]. Therefore, we can separate the effects of axial and lateral misalignments with wavefront measurement at only one field point (wavefront measurements at multiple field positions are needed when solving the specific values of lateral misalignments). The underlying reason we can separate these two effects is that the relationship between astigmatism and coma induced by axial misalignments is different from those induced by lateral misalignments.

Monte Carlo simulation will be performed to demonstrate the accuracy of the axial misalignment calculated with the proposed method. Three cases will be considered in the Monte Carlo simulation, and the specific ranges for different misalignment parameters in each case are shown in Table 1. In case 1 and case 2, the misalignment ranges increase progressively but no measurement errors are considered. Case 3 has the same misalignment ranges as case 2, while it further includes 3% measurement errors, i.e., a relative 3% of the measurement errors in plus or minus are randomly added to the wavefront Fringe Zernike coefficients read from the optical simulation software [23].

For each case, 100 misalignment states are randomly generated following a standard normal distribution. The root mean square deviation (RMSD) between the introduced axial misalignments and the calculated axial misalignments under these 100 misalignment states is utilized to evaluate the calculation accuracy, which can be expressed as

$$\mathrm{RMSD} = \sqrt{\frac{1}{N}\sum_{n=1}^{N}[D(n) - d(n)]^2}, \quad (34)$$

where $D(n)$ represents the calculated misalignments, $d(n)$ represents the introduced misalignments, and $N = 100$. The simulation results for these three cases are shown in Table 2.

Table 2. RMSDs of the Calculated Axial Misalignment of the SM for the Three Cases

	Case 1	Case 2	Case 3
RMSD (mm)	0.0227	0.0418	0.0512

We can see from Table 2 that the proposed model can decouple axial misalignments from lateral misalignments and quantitatively calculate the value of axial misalignment of the SM. We can also find that the accuracy of the calculated axial misalignment decreases with the increase in the misalignment range. The main reason for this is that the decoupling model is proposed based on the third-order NAT. We only consider third-order aberrations of the on-axis parent system, while the higher-order aberrations of the misaligned on-axis system can also be converted to a series of lower-order aberrations through pupil coordinate transformation. However, the expression of the calculation model in this section is very simple, which can contribute to a better understanding of the mechanism of separating the two kinds of misalignments.

7. CONCLUSION

This paper presents an in-depth and systematic discussion on the interactions between the effects of axial and lateral misalignments in off-axis two-mirror astronomical telescopes. The aberration function of this class of telescopes in the presence of axial and lateral misalignments is derived. The specific expressions of two dominant non-rotationally symmetric aberrations, i.e., astigmatism and coma, are obtained and the aberration field characteristics are discussed. The mutual compensation between axial and lateral misalignments is discussed. Finally, one problem of aberration compensation is pointed out and explained, and an analytic method of decoupling these two kinds of misalignments is further proposed. Most of this work can be extended to other kinds of pupil-offset off-axis astronomical telescopes, such as off-axis TMA telescopes. Some important results of this work are presented below:

(1) It is shown that under certain conditions a node will arise in the field of view for astigmatism and coma in the presence of both kinds of misalignments, while typically no node exists in the field of view with only one kind of misalignment. The underlying reason for this is that the field-constant aberration terms induced by the axial and lateral misalignment can compensate each other.

(2) It is shown that the individual astigmatic or coma aberration field induced by axial misalignments can well be compensated with lateral misalignments, while axial misalignment can only compensate 0° astigmatism and 90° coma induced by lateral misalignments.

(3) An analytic method is proposed to decouple axial misalignments from lateral misalignments and quantitatively calculate the value of axial misalignment of the SM with wavefront measurement at one field position. The underlying reason we can separate these two effects is that the relationship between astigmatism and coma induced by axial misalignments is different from the relationship between astigmatism and coma induced by lateral misalignments.

We should also point out that this paper mainly focuses on providing some intuitive understanding and valuable insights into the interactions between axial and lateral misalignments, and that the mathematical accuracy is actually not very high. To describe the effects of axial and lateral misalignments more accurately, we need to consider the high-order aberrations of the on-axis parent system, which will generate some aberration contributions in the off-axis system through pupil coordinate transformation. Furthermore, while wavefront measurements at only one field position are enough to separate the effects of axial and lateral misalignments, wavefront measurements and more field points are needed if we want to determine the value of lateral misalignments.

Funding. National Key Research and Development Program (2016YFE0205000); National Natural Science Foundation of China (NSFC) (61705223, 61905241).

REFERENCES

1. R. J. R. Kuhn and S. L. Hawley, "Some astronomical performance advantages of off-axis telescopes," Publ. Astron. Soc. Pac. **111**, 601–620 (1999).
2. F. Zeng, X. Zhang, J. Zhang, G. Shi, and H. Wu, "Optics ellipticity performance of an unobscured off-axis space telescope," Opt. Express **22**, 25277–25285 (2014).
3. G. Moretto and J. R. Kuhn, "Optical performance of the 6.5-m off-axis new planetary telescope," Appl. Opt. **39**, 2782–2789 (2000).
4. M. A. Lundgren and W. L. Wolfe, "Alignment of a three-mirror off-axis telescope by reverse optimization," Opt. Eng. **30**, 307–311 (1991).
5. G. Ju, C. Yan, Z. Gu, and H. Ma, "Nonrotationally symmetric aberrations of off-axis two-mirror astronomical telescopes induced by axial misalignments," Appl. Opt. **57**, 1399–1409 (2018).
6. G. Ju, C. Yan, Z. Gu, and H. Ma, "Aberration fields of off-axis two-mirror astronomical telescopes induced by lateral misalignments," Opt. Express **24**, 24665–24703 (2016).
7. G. Ju, H. Ma, Z. Gu, and C. Yan, "Experimental study on the extension of nodal aberration theory to pupil-offset off-axis three-mirror anastigmatic telescopes," J. Astron. Telesc. Instrum. Syst. **5**, 029001 (2019).
8. G. Ju, H. Ma, and C. Yan, "Aberration fields of off-axis astronomical telescopes induced by rotational misalignments," Opt. Express **26**, 24816–24834 (2018).
9. J. C. Wyant and K. Creath, "Basic wavefront aberration theory for optical metrology," in *Applied Optics and Optical Engineering*, R. R. Shannon and J. C. Wyant, eds. (Academic, 1992), pp. 1–53.
10. R. V. Shack and K. P. Thompson, "Influence of alignment errors of a telescope system," Proc. SPIE **251**, 146–153 (1980).
11. R. A. Buchroeder, "Tilted component optical systems," Ph.D. dissertation (University of Arizona, 1976).
12. K. P. Thompson, "Aberration fields in tilted and decentered optical systems," Ph.D. dissertation (University of Arizona, 1980).
13. K. P. Thompson, "Description of the third-order optical aberrations of near-circular pupil optical systems without symmetry," J. Opt. Soc. Am. A **22**, 1389–1401 (2005).
14. K. P. Thompson, T. Schmid, O. Cakmakci, and J. P. Rolland, "Real-ray-based method for locating individual surface aberration field centers in imaging optical systems without rotational symmetry," J. Opt. Soc. Am. A **26**, 1503–1517 (2009).
15. T. Schmid, K. P. Thompson, and J. P. Rolland, "Misalignment-induced nodal aberration fields in two-mirror astronomical telescopes," Appl. Opt. **49**, D131–D144 (2010).
16. K. P. Thompson, T. Schmid, and J. P. Rolland, "The misalignment induced aberrations of TMA telescopes," Opt. Express **16**, 20345–20353 (2008).
17. J. Wang, B. Guo, Q. Sun, and Z. Lu, "Third-order aberration fields of pupil decentered optical systems," Opt. Express **20**, 11652–11658 (2012).
18. H. H. Hopkins, *The Wave Theory of Aberrations* (Oxford, 1950).
19. H. Ma, G. Ju, and X. Zhang, "Optical design method of two-mirror astronomical telescopes with reduced misalignment sensitivities based on the nodal aberration theory," OSA Continuum **1**, 145–161 (2018).
20. J. R. Meyer-Arendt, in *Introduction to Classical and Modern Optics*, 2nd ed.(Pearson, 1972), Part 2, pp. 208–211.
21. L. Didkovsky, J. Kuhn, and P. Goode, "Optical design for a new off-axis 1.7-m solar telescope (NST) at Big Bear," Proc. SPIE **5171**, 333–343 (2004).
22. R. K. Tyson, "Conversion of Zernike aberration coefficients to Seidel and high-order power-series aberration coefficients," Opt. Lett. **7**, 262–264 (1982).
23. G. Ju, C. Yan, Z. Gu, and H. Ma, "Computation of astigmatic and trefoil figure errors and misalignments for two-mirror telescopes using nodal-aberration theory," Appl. Opt. **55**, 3373–3386 (2016).